

## NEUROSYSTEMS

# Dopaminergic axons in different divisions of the adult rat striatal complex do not express vesicular glutamate transporters

Jonathan Moss,<sup>1</sup> Mark A. Ungless<sup>2</sup> and J. Paul Bolam<sup>1</sup>

<sup>1</sup>Medical Research Council Anatomical Neuropharmacology Unit, Department of Pharmacology, University of Oxford, Oxford, UK

<sup>2</sup>Medical Research Council Clinical Sciences Centre, Imperial College, Hammersmith Hospital, London, UK

**Keywords:** basal ganglia, glutamatergic, mesostriatal, nigrostriatal, nucleus accumbens, striatum

## Abstract

Midbrain dopamine neurons signal rapid information about rewards and reward-related events. It has been suggested that this fast signal may, in fact, be conveyed by co-released glutamate. Evidence that dopamine neurons co-release glutamate comes largely from studies involving cultured neurons or tissue from young animals. Recently, however, it has been shown that this dual glutamatergic/dopaminergic phenotype declines with age, and can be induced by injury, suggesting that it is not a key feature of adult dopamine neurons. Here, we provide further support for this view by showing that dopaminergic axons and terminals in subregions of the adult striatum do not express vesicular glutamate transporters (VGluT1, VGluT2 or VGluT3). Striatal tissue from the adult rat was immunolabelled to reveal tyrosine hydroxylase (TH; biosynthetic enzyme of dopamine) and one of the three known VGluTs. Importantly, we compared the immunogold labelling for each of the VGluTs associated with TH-positive structures with background labelling at the electron microscopic level. In addition, we carried out a subregional analysis of the core and shell of the nucleus accumbens. We found that dopaminergic axons and terminals in the dorsolateral striatum and ventral striatum (nucleus accumbens core and shell) do not express VGluT1, VGluT2 or VGluT3. We conclude, therefore, that in the normal, adult rat striatum, dopaminergic axons do not co-release glutamate.

## Introduction

Midbrain dopamine neurons play central roles in reward processing, and their dysfunction is implicated in a range of neurological and psychiatric disorders. It has been suggested that midbrain dopamine neurons co-release glutamate, which has important implications for our understanding of their function (for discussion see Rayport, 2001; Sulzer & Rayport, 2000; Lapish *et al.*, 2007). In particular, it has been argued that glutamate may convey their rapid reward-related signal (for discussion see Lapish *et al.*, 2007), which occurs with a latency and duration of 100–200 ms (Schultz, 1998).

The possibility of glutamate co-release was originally raised by the observation that dopamine neurons express phosphate-activated glutaminase, the biosynthetic enzyme for the neurotransmitter glutamate (Kaneko *et al.*, 1990). In addition, stimulation of the substantia nigra pars compacta evoked fast excitatory synaptic events in striatal neurons (Kitai *et al.*, 1976). This was followed by the striking observations that individual dopamine neurons in culture form functional glutamatergic autapses (Sulzer *et al.*, 1998) and synapses onto co-cultured striatal neurons (Joyce & Rayport, 2000). Moreover, in *ex vivo* brain slices, with the mesoaccumbens pathway partly intact,

glutamatergic synaptic events can be evoked by stimulating cell bodies in the ventral tegmental area (VTA) (Chuhma *et al.*, 2004).

The co-release hypothesis makes two key predictions. First, dopamine neuron cell bodies should express mRNA for one or more vesicular glutamate transporters (VGluTs). However, although the majority of cultured dopamine neurons express VGluT2 (Dal Bo *et al.*, 2008), co-expression in adult dopamine neurons has been reported to be extremely limited (Kawano *et al.*, 2006; Yamaguchi *et al.*, 2007; Nair-Roberts *et al.*, 2008). Moreover, these studies have provided evidence for a discrete population of glutamatergic (non-dopaminergic) neurons within the rostral-medial VTA (Kawano *et al.*, 2006; Yamaguchi *et al.*, 2007; Nair-Roberts *et al.*, 2008), which may be responsible for the excitatory events evoked in the striatum by stimulation of the VTA (e.g. Chuhma *et al.*, 2004). Mendez *et al.* (2008) report not only that culturing of dopamine neurons induces VGluT2 expression, but also that its *in vivo* expression declines with age. Furthermore, 6-hydroxydopamine lesions increase co-expression of VGluT and tyrosine hydroxylase (TH) in the VTA and substantia nigra pars compacta (Dal Bo *et al.*, 2008; Bérubé-Carrière *et al.*, 2009). Taken together, these results suggest that dopamine neurons only express mRNA for the VGluTs early in development, or following injury.

The second key prediction that the co-release hypothesis makes is that dopaminergic terminals in target regions, including the striatum, should be immunopositive for VGluTs. However, as for mRNA in the

Correspondence: Jonathan Moss, <sup>1</sup>Medical Research Council Anatomical Neuropharmacology Unit, as above.  
E-mail: j.moss@mail.com

Received 5 March 2010, revised 9 December 2010, accepted 16 December 2010

cell bodies, it appears that VGluT2 protein is expressed only in younger animals or following injury (Dal Bo *et al.*, 2008; Descarries *et al.*, 2008; Bérubé-Carrière *et al.*, 2009). In these studies, however, VGluT labelling was not compared with background, so it is possible that low levels of VGluT immunolabelling were merely reflective of background labelling. We therefore sought to address this issue by conducting a thorough assessment of background labelling in subregions of the striatum and by direct comparison with non-dopaminergic terminals forming asymmetrical synapses. In addition, these previous studies have analysed the core, but not the shell, of the nucleus accumbens. This may be important because, in brain slices, VTA stimulation is particularly effective at evoking glutamatergic synaptic responses in the ventromedial shell of the nucleus accumbens (e.g. Chuhma *et al.*, 2009). We therefore conducted a subregional analysis, to include the shell of the nucleus accumbens. The results of this study have previously been reported in abstract form (Moss & Bolam, 2009a,b).

## Materials and methods

### Tissue preparation

Twelve male adult Sprague–Dawley rats [postnatal day (P)42–98 and 294–425 g; Charles River, Margate, UK] were perfused-fixed with 200 mL of fixative (3% paraformaldehyde, 0.1% glutaraldehyde in 0.1 M phosphate buffer, pH 7.4) over approximately 25 min. Their brains were cut into sagittal sections on a vibrating vibratome, freeze-thawed, and incubated in 10% normal goat serum (NGS) in phosphate-buffered saline (PBS). All experiments were conducted in accordance with the Animals (Scientific Procedures) Act 1986 (UK).

### Immunohistochemistry

Sections containing dorsolateral striatum (DLS), nucleus accumbens core (NAC) and nucleus accumbens shell (NAS) were selected (Paxinos & Watson, 2007) and double-immunolabelled to reveal TH and one of VGluT1, VGluT2 or VGluT3 by immunoperoxidase and immunogold methods, respectively, as described previously (Moss & Bolam, 2008). Of the 12 animals used, animals 1–3 were used to examine VGluT1 in the DLS, animals 4–6 to examine VGluT2 in the DLS, animals 7–9 to examine VGluT1 and VGluT2 in the NAC and NAS, and animals 10–12 to examine VGluT3 in all regions. In brief, sections from three animals were each incubated with antibodies against VGluT1, VGluT2 or VGluT3 [VGluT1, raised in rabbits (MAb Technologies, Stone Mountain, GA, USA); VGluT2, raised in rabbits (Synaptic Systems, Göttingen, Germany); and VGluT3, raised in guinea pigs (Millipore, Molsheim, France)] at a dilution of 1 : 2000 in 2% NGS-PBS overnight. Antigenic sites were revealed with secondary antibodies conjugated to colloidal gold [1.4-nm gold particles (Nanoprobes, Yaphank, NY, USA); 1 : 100 in 1% NGS-PBS] with subsequent silver intensification [HQ Silver kit (Nanoprobes); silver-intensified immunogold particles are hereafter simply referred to as immunogold particles]. The distribution of immunolabelling at the light and electron microscopic levels was distinct for each primary antibody, and consistent with previous observations (Fremeau *et al.*, 2002; Dal Bo *et al.*, 2004, 2008; Fujiyama *et al.*, 2004; Herzog *et al.*, 2004; Lacey *et al.*, 2005; Descarries *et al.*, 2008; Moss & Bolam, 2008).

All sections were then incubated with a mouse monoclonal antibody raised against TH (Sigma; 1 : 1000 in 2% NGS-PBS), followed by a biotinylated secondary antibody [BA9200 (Vector Laboratories,

Peterborough, UK); diluted 1 : 200 in 1% NGS-PBS] and then avidin–biotin–peroxidase complex (Vector Laboratories), before being revealed by a peroxidase reaction, with diaminobenzidine (DAB) as the chromogen. They were treated with osmium tetroxide (7 min, 1% in 0.1 M phosphate buffer, pH 7.4), dehydrated through a series of dilutions of ethanol (50%, 70% with 1% uranyl acetate, 95% and 100%) and propylene oxide, and placed into resin overnight. The sections were then mounted onto slides, coverslips were applied, and the resin was cured at approximately 65 °C over three nights. Tissue from the three striatal regions was removed from slides, and 50-nm serial sections were cut, collected onto pioloform-coated, single-slot copper grids, and lead-stained to improve contrast for electron microscopic examination. Omitting primary antibodies in turn, but carrying out the rest of the double-labelling procedure, resulted in a complete lack of peroxidase or immunogold labelling for TH and VGluT, respectively. Omitting secondary antibodies individually demonstrated that immunolabelling could not be a result of cross-reactivity.

### Electron microscopic analysis

A Philips CM10 electron microscope was used to examine TH-immunopositive axons in each striatal region for the presence of immunogold particles identifying the VGluTs. The TH immunolabelling also identifies noradrenergic structures, but these are scarce in the DLS and only slightly more common in the ventral striatum (Carlsson, 1959; Moore & Card, 1984). Analyses were performed at a minimum of 5 µm from the tissue–resin border (i.e. the surface of the section). The maximum distance from the tissue–resin border examined was determined by the penetration of the gold-conjugated antibody together with the angle at which the tissue–resin was sectioned, and was therefore variable. Fifty electron micrograph frames were randomly selected for analysis from each striatal area (DLS, NAC and NAS) for each staining protocol (VGluT1, VGluT2 or VGluT3 with TH) in three animals for each (a total of 27 sets of 50 frames). This was carried out by selecting a random serial section from a set of six, selecting a random point within this section at a magnification of × 6200, increasing the magnification to between × 54 100 and × 99 100, and digitally recording the image (Gatan multiscan CCD camera; Gatan, Abingdon, UK). Analyses were performed on the digital images with the publicly available software IMAGEJ ([rsb.info.nih.gov/ij/](http://rsb.info.nih.gov/ij/)); brightness and contrast functions were used to separate the VGluT-positive immunogold labelling from the TH-positive DAB peroxidase labelling when the two occurred in the same structures, thus preventing the possibility that the DAB reaction product obscured the immunogold particles. The number of immunogold particles within each TH-positive structure in these series of 50 frames was then quantified (approximately 1546 µm<sup>2</sup> for each VGluT in each region). As a control, the same micrographs were used to assess the numbers of immunogold particles overlying structures known not to express VGluTs, namely dendritic spines. The numbers and proportions of both TH-positive structures and dendritic spines containing immunogold labelling were examined and compared (paired *t*-test) for each striatal region (Table 1; Fig. 2).

The mean densities of gold immunolabelling for VGluTs overlying TH-positive structures were also calculated (Table 1; Fig. 3). These densities were calculated for each structure on the basis of the number of gold particles that it contained and the mean area of a sample of TH-positive structures of that specific animal, region and VGluT labelling (sample composed of about 23 structures from an area of 378 µm<sup>2</sup> per animal, region and VGluT labelling, 623 in

TABLE 1. Immunogold labelling for VGluT1–3 in TH-positive structures, dendritic spines and asymmetrical synapse-forming terminals of the DLS, NAC and NAS

VGluT and striatal region	Number of structures examined			Mean density (all structures) per $\mu\text{m}^2 \pm \text{SEM}$		Mean number of each structure labelled $\pm \text{SEM}$ (% mean $\pm \text{SEM}$ )		Mean density (labelled structures) per $\mu\text{m}^2 \pm \text{SEM}$		
	TH	Sp.	Asym.	TH	Sp.	TH	Sp.	TH	Sp.	Asym.
VGluT1 DLS	425	369	42	0.60 $\pm$ 0.24	1.27 $\pm$ 0.30	6 $\pm$ 3 (4 $\pm$ 1)	10 $\pm$ 1 (8 $\pm$ 1)	14 $\pm$ 3	16 $\pm$ 4	72 $\pm$ 16
VGluT2 DLS	383	350	33	1.20 $\pm$ 1.16	2.99 $\pm$ 1.00	4 $\pm$ 4 (5 $\pm$ 5)	17 $\pm$ 2 (15 $\pm$ 3)	12 $\pm$ 7	19 $\pm$ 4	114 $\pm$ 12
VGluT3 DLS	267	348	–	0.32 $\pm$ 0.09	1.08 $\pm$ 0.54	3 $\pm$ 1 (3 $\pm$ 1)	5 $\pm$ 3 (4 $\pm$ 2)	12 $\pm$ 2	17 $\pm$ 9	–
VGluT1 NAC	304	295	41	0.53 $\pm$ 0.13	1.11 $\pm$ 0.52	6 $\pm$ 1 (5 $\pm$ 1)	5 $\pm$ 1 (5 $\pm$ 1)	10 $\pm$ 1	19 $\pm$ 4	50 $\pm$ 12
VGluT2 NAC	278	401	69	0.91 $\pm$ 0.42	1.16 $\pm$ 0.40	6 $\pm$ 3 (6 $\pm$ 3)	10 $\pm$ 3 (8 $\pm$ 3)	13 $\pm$ 3	16 $\pm$ 4	45 $\pm$ 5
VGluT3 NAC	365	372	–	0.15 $\pm$ 0.07	1.01 $\pm$ 0.23	1 $\pm$ 1 (1 $\pm$ 1)	7 $\pm$ 1 (5 $\pm$ 0)	9 $\pm$ 5	18 $\pm$ 3	–
VGluT1 NAS	299	298	36	1.02 $\pm$ 0.72	0.87 $\pm$ 0.40	5 $\pm$ 2 (5 $\pm$ 2)	5 $\pm$ 3 (6 $\pm$ 3)	16 $\pm$ 6	19 $\pm$ 5	49 $\pm$ 6
VGluT2 NAS	217	272	43	0.86 $\pm$ 0.43	2.07 $\pm$ 0.91	8 $\pm$ 3 (11 $\pm$ 4)	9 $\pm$ 5 (7 $\pm$ 4)	7 $\pm$ 1	23 $\pm$ 6	78 $\pm$ 14
VGluT3 NAS	256	269	–	0.14 $\pm$ 0.01	0.28 $\pm$ 0.11	1 $\pm$ 0 (1 $\pm$ 0)	2 $\pm$ 1 (2 $\pm$ 1)	11 $\pm$ 1	15 $\pm$ 1	–

Data for each VGluT and striatal region are shown as means of the three animals examined  $\pm$  SEMs to show animal-to-animal variability. The numbers of TH-positive structures (TH) and dendritic spines (Sp.) examined for each are shown, together with the mean densities of immunogold labelling, when either all structures are taken into account or when only those structures labelled with at least one gold particle are taken into account. The numbers and percentages of TH-positive structures and spines labelled with gold particles are also shown. The densities of labelling in only those TH-positive structures and spines labelled with immunogold particles are displayed, together with the densities of VGluT1-positive and VGluT2-positive terminals forming asymmetrical synapses (Asym.) for comparison. By definition, the number of VGluT1-positive and VGluT2-positive terminals examined were the number that were labelled. Terminals forming asymmetrical synapses do not contain VGluT3 labelling so no values are shown.

total; density = number of gold particles/mean area of structures). These individual structure densities were then used to calculate means and standard errors of the mean (SEMs) for each animal (Table 1; Fig. 3). The means for each region and VGluT labelling were then calculated from the three individual animal means with SEMs to show animal-to-animal variability (Table 1; Fig. 3). Similar density calculations were performed for dendritic spines for the purpose of comparison (VGluT1 and VGluT2, one-way ANOVA with Tukey's *post hoc* test; VGluT3, paired *t*-test; Table 1; Fig. 3). The dendritic spines measured to ascertain the mean area of dendritic spines for each animal, region and VGluT labelling came from the same electron micrograph that were analysed for the mean area of TH-positive structures (sample of approximately 24 spines per animal, region and VGluT labelling, 641 in total). As an additional comparison, the mean densities of VGluT immunogold particles in VGluT1-immunolabelled and VGluT2-immunolabelled terminals forming asymmetrical synapses were measured for each animal, region and either VGluT1 or VGluT2 labelling ( $n = 119$  for VGluT1 and  $n = 145$  for VGluT2 in total; Fig. 3). These densities were compared (one-way ANOVA with Tukey's *post hoc* test) against the mean densities of only the TH-positive structures and spines that were labelled, as the asymmetrical synapse-forming terminals were, by definition, labelled. The mean densities for asymmetrical synapse-forming terminals of the three animals for each region and VGluT1 or VGluT2 are shown with SEMs to reflect animal-to-animal variability (Table 1; Fig. 3). Corrections for shrinkage of the tissue were not made.

## Results

### *The relative densities of immunolabelling for TH and VGluT1–3*

The distribution and form of peroxidase immunolabelling for TH were consistent with previous observations at the light and electron microscopic levels. Thus, the striatum and both divisions of the nucleus accumbens were densely innervated by TH-positive fibres and, at the electron microscopic level, contained numerous profiles that often contained synaptic vesicles and formed symmetrical synapses (Hanley & Bolam, 1997; Moss & Bolam, 2008). Similarly, immunogold labelling for VGluT1 and VGluT2 was consistent with

previous studies (Dal Bo *et al.*, 2004, 2008; Fujiyama *et al.*, 2004; Lacey *et al.*, 2005; Descarries *et al.*, 2008; Moss & Bolam, 2008). The striatal complex was densely labelled with punctate structures that, when examined at the electron microscopic level, consisted of preterminal axons and terminal axons forming asymmetrical synapses, densely overlaid with immunogold particles (Fig. 1A and B). The mean densities ( $\pm$  SEM) for VGluT1 labelling in terminals were 72  $\pm$  16, 50  $\pm$  12 and 49  $\pm$  6 immunogold particles/ $\mu\text{m}^2$  in the DLS, NAC and NAS, respectively ( $n = 119$ ; Table 1). The mean densities ( $\pm$  SEM) for VGluT2 labelling in terminals were 114  $\pm$  12, 45  $\pm$  5 and 78  $\pm$  14 immunogold particles/ $\mu\text{m}^2$  in the DLS, NAC and NAS, respectively ( $n = 145$ ; Table 1). Immunogold labelling for VGluT3 was, in general, much more sparse than that for VGluT1 and VGluT2 in all regions of the striatum examined (Fig. 1C), with fewer than 10 gold particles typically being present in 12.6- $\mu\text{m}^2$  electron micrograph frames. Labelling was chiefly seen in vesicle-filled axonal processes, but also in cell bodies and dendritic shafts. This labelling is consistent with previous studies (Fremeau *et al.*, 2002; Herzog *et al.*, 2004) and is likely to reflect the VGluT3-expressing cholinergic interneurons of the striatum; cell bodies labelled for VGluT3 are large and sparsely distributed (Herzog *et al.*, 2004) and also express choline acetyltransferase (Fremeau *et al.*, 2002).

### *Low levels of VGluT immunolabelling in TH-positive structures*

To determine whether dopaminergic axons in the DLS, NAC and NAS express VGluTs, tissue double-labelled by the immunogold and immunoperoxidase methods to reveal the VGluTs and TH, respectively, was examined at the electron microscopic level. In randomly selected electron micrographs, the frequency of occurrence, number and density of VGluT immunogold particles within TH-positive structures were quantified (Table 1; Figs 2 and 3). In the same data set, the frequency of occurrence, number and density of VGluT immunogold particles within dendritic spines were also quantified (Table 1; Figs 2 and 3). As medium spiny neurons in the striatum do not express any of the VGluTs (Fremeau *et al.*, 2001, 2002; Herzog *et al.*, 2004) and account for the vast majority of dendritic spines, the values observed serve to quantify the levels of non-specific or background labelling.

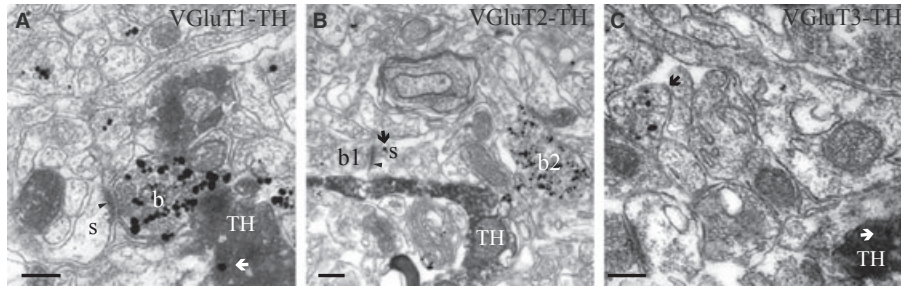


FIG. 1. The distribution of VGluT immunogold labelling in TH-positive structures and dendritic spines is similar and substantially less than that in excitatory boutons forming asymmetrical synapses. (A) An excitatory bouton (b) containing multiple VGluT1 immunogold particles makes an asymmetrical synaptic contact (arrowhead) with a dendritic spine (s). Lying beneath the axon is a TH-positive structure (TH) that contains a single gold particle (arrow); this is typical of the level of labelling seen in all tissue examined. (B) A dendritic spine (s) postsynaptic to a bouton (b1) contains two VGluT2 immunogold particles (arrow); this is typical of the levels of background labelling seen in dendritic spines and similar to the levels seen in TH-positive structures. In the vicinity is a VGluT1-positive excitatory bouton (b2) that contains multiple gold particles, and a TH-positive structure (TH) that is devoid of gold particles. (C) Typically sparse immunogold labelling for VGluT3, most commonly found in vesicle-filled axonal processes (black arrow), one particle of which (white arrow) is seen overlying a TH-positive structure (TH). Scale bars – 0.2  $\mu\text{m}$ .

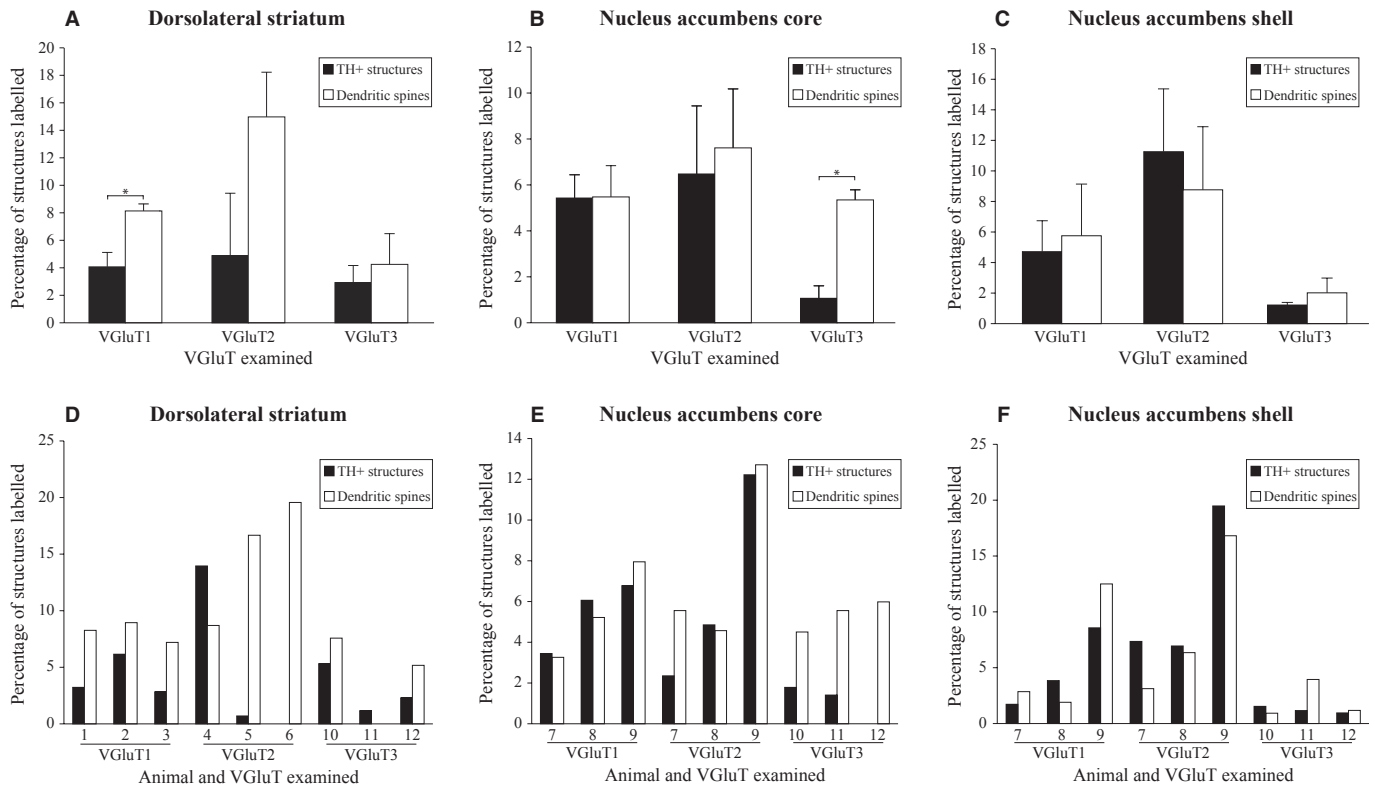


FIG. 2. TH-positive structures do not contain more immunogold labelling for VGluTs than background levels observed in dendritic spines. The mean percentages ( $\pm$  SEMs; three animals each) of TH structures and dendritic spines labelled with immunogold for VGluT1, VGluT2 and VGluT3 in the DLS (A), NAC (B) and NAS (C). Statistical comparisons were made with paired *t*-tests (statistical differences are shown by \* $P < 0.05$ ; for exact *P*-values, see text), and the numbers used to calculate each percentage can be found in Table 1. The percentages for each individual animal, from which the means were calculated, are shown beneath the mean data for each corresponding striatal region (D–F).

Overall, the analysis of 2794 TH-positive profiles over the three striatal regions in three rats revealed that a very small proportion were associated with VGluT immunogold particles (VGluT1, 4.9%, 50/1028; VGluT2, 6.4%, 56/878; VGluT3, 1.7%, 15/888; all VGluTs, 4.3%, 121/2794). Proportions for VGluT1, VGluT2 and VGluT3, respectively, ranged from  $4 \pm 1\%$  to  $5 \pm 2\%$ ,  $5 \pm 5\%$  to  $11 \pm 4\%$  and  $1 \pm 0\%$  to  $3 \pm 1\%$  over the three striatal regions (mean  $\pm$  SEM; Table 1; Fig. 2). Significantly more profiles contained a single immunogold particle (74/2794) than two or more (47/2794;  $\chi^2 = 6.2$ ,

$P = 0.013$ ). This represented an overall density of between  $0.14 \pm 0.01$  and  $1.20 \pm 1.16$  immunogold particles/ $\mu\text{m}^2$  for each VGluT and striatal region (mean  $\pm$  SEM; Table 1) or, when only considering those structures that were associated with immunogold particles,  $7 \pm 1$  to  $16 \pm 6$  particles/ $\mu\text{m}^2$  (mean  $\pm$  SEM; Table 1; Fig. 3A–C).

Considering each of the striatal regions separately, the highest levels of labelling were seen for VGluT2 in the NAC, where  $11 \pm 4\%$  of the TH-positive structures were associated with immunogold particles (Table 1; Fig. 2C). However, this proportion represents 25 structures

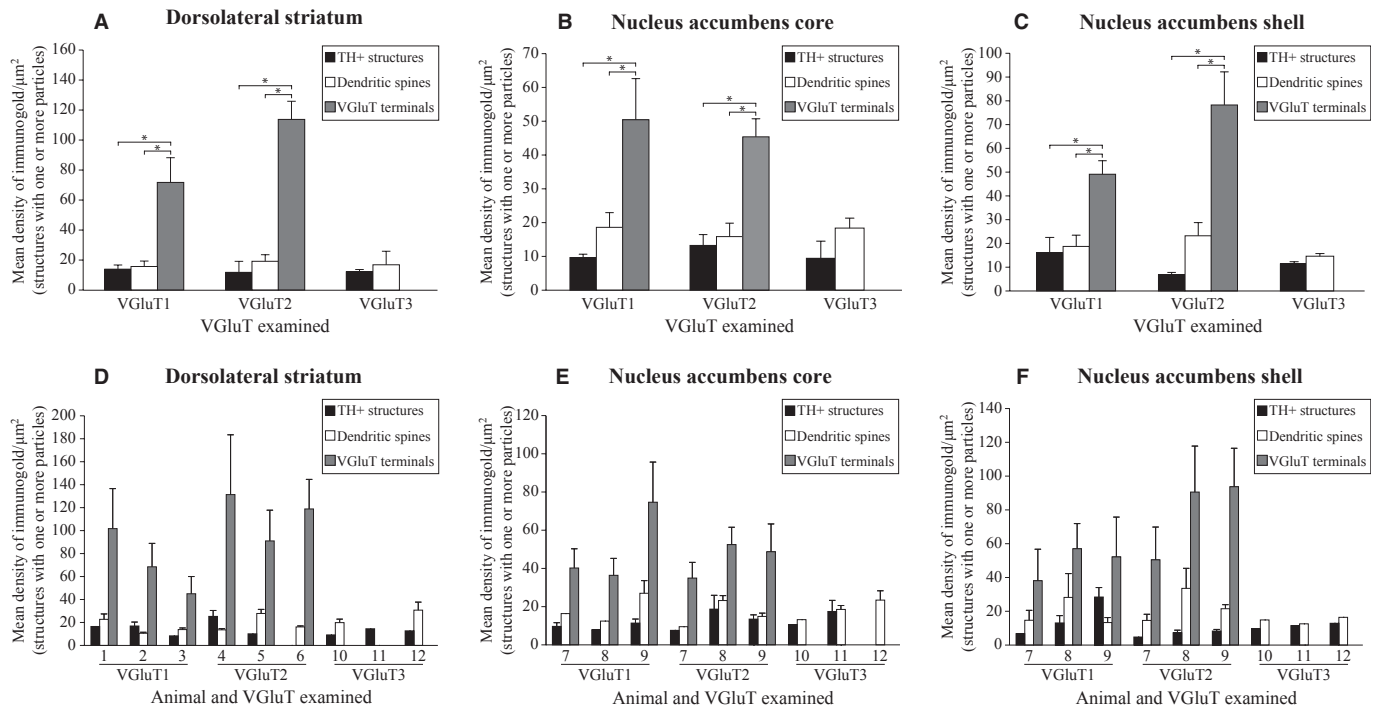


FIG. 3. Mean densities of VGluT immunogold labelling observed in TH-positive structures are no different from background densities seen in dendritic spines and are significantly less than densities seen in VGluT1-positive or VGluT2-positive, asymmetrical synapse-forming terminals. The mean densities ( $\pm$  SEMs; three animals each) of VGluT1, VGluT2 or VGluT3 immunogold labelling observed in VGluT-labelled TH-positive structures and dendritic spines in the DLS (A), NAC (B) and NAS (C) and mean densities of VGluT1 and VGluT2 immunogold labelling in asymmetrical synapse-forming terminals immunopositive for these VGluTs. Statistical comparisons were made with one-way ANOVA with Tukey's *post hoc* test (VGluT1 and VGluT2) or paired *t*-test (VGluT3; statistical differences are shown by  $*P < 0.05$ ). The numbers relating to these mean densities can be found in Table 1. The densities ( $\pm$  SEMs) for each individual animal, from which mean densities were calculated, are shown beneath the mean data for each corresponding striatal region (D–F).

of 217 examined; 13 contained one gold particle, six contained two particles, five contained three particles, and one contained four particles. For excitatory terminals that form asymmetrical synapses in the same striatal region, the mean number of gold particles per terminal was  $18 \pm 4$ , with a range of 1–73 particles (16 of the 43 examined contained five gold particles or fewer, but 11 contained over 30). The density of VGluT1 and VGluT2 immunogold associated with immunogold-labelled TH-positive structures was lower than that of immunogold-labelled excitatory terminals when the two were compared within the same striatal regions (one-way ANOVA with Tukey's *post hoc* test,  $P < 0.05$ ; Fig. 3A–C).

#### Background levels of VGluT immunolabelling match or exceed those seen in TH-positive structures

Although we observed only low numbers of immunogold particles associated with TH-positive structures in comparison with excitatory terminals, the labelling may, in fact, reflect low levels of the VGluTs. In order to control for this, background immunolabelling was analysed in dendritic spines that lack vesicles and thus also lack VGluTs. Seven per cent of dendritic spines were associated with immunogold labelling for VGluT1–3 (208/2974; VGluT1, 6.4%, 62/962; VGluT2, 10.3%, 105/1023; VGluT3, 4.1%, 41/989). Proportions for each VGluT in each striatal area ranged from  $5 \pm 1\%$  to  $8 \pm 1\%$ ,  $7 \pm 4\%$  to  $15 \pm 3\%$  and  $2 \pm 1\%$  to  $5 \pm 0\%$  for VGluT1, VGluT2 and VGluT3, respectively (Table 1; Fig. 2A–C). Background levels of immunogold labelling for each VGluT were similar to, or higher than, the levels in TH-positive structures of the same striatal region (paired *t*-test; DLS, VGluT1,  $t = 6.097$ ,  $P = 0.0259$ ; DLS, VGluT2,  $t = 1.303$ ,

$P = 0.3224$ ; DLS, VGluT3,  $t = 1.053$ ,  $P = 0.4026$ ; NAC, VGluT1,  $t = 0.08091$ ,  $P = 0.9429$ ; NAC, VGluT2,  $t = 1.075$ ,  $P = 0.3948$ ; NAC, VGluT3,  $t = 4.534$ ,  $P = 0.0454$ ; NAS, VGluT1,  $t = 0.6136$ ,  $P = 0.6020$ ; NAS, VGluT2,  $t = 2.373$ ,  $P = 0.1410$ ; NAS, VGluT3,  $t = 0.7816$ ,  $P = 0.5163$ ; Fig. 2A–C).

As was the case for the TH-positive structures, significantly more spines contained one immunogold particle (161/2974) than greater numbers of gold particles (47/2974;  $\chi^2 = 64.7$ ,  $P = 8.5 \times 10^{-16}$ ). The density of immunolabelling for each VGluT in dendritic spines ranged from  $0.28 \pm 0.11$  to  $2.99 \pm 1.00$  immunogold particles/ $\mu\text{m}^2$ , and when considering only immunogold-labelled spines, densities of labelling for VGluTs ranged from  $15 \pm 1$  to  $23 \pm 6$  immunogold particles/ $\mu\text{m}^2$  (Table 1). These densities were similar to those of TH-positive structures (VGluT1 and VGluT2, one-way ANOVA with Tukey's *post hoc* test,  $P > 0.05$ , and VGluT3, paired *t*-test – DLS,  $t = 0.49$ ,  $P = 0.673$ ; NAC,  $t = 1.25$ ,  $P = 0.338$ ; NAS,  $t = 2.69$ ,  $P = 0.115$ ; Fig. 3A–C).

Taken together, the data thus show that specific immunoreactivity for VGluT1, VGluT2 or VGluT3 is not present in TH-positive structures of the adult rat striatum, and suggest that dopaminergic axons of this region do not contain vesicular glutamate transporters, or express them at levels below detectability.

#### Discussion

We show here that, in the adult rat striatum, immunolabelling for vesicular glutamate transporters associated with dopaminergic structures is equivalent to, or less than, background labelling. In particular, we show that this is the case for the DLS, the NAC and the NAS.

Moreover, we have carefully examined background labelling to establish that our methods are sensitive enough to detect even low levels of labelling. We therefore conclude that dopaminergic structures in the dorsolateral and ventral striatum of the adult rat do not express VGluT1, VGluT2 or VGluT3. Because the expression of a VGluT is a prerequisite for a structure to accumulate glutamate in vesicles (Bellocchio *et al.*, 2000; Freneau *et al.*, 2001, 2002; Takamori *et al.*, 2001), it is likely that the vesicular release of glutamate does not occur from dopaminergic neurons in the adult forebrain.

With the use of similar methods to those used in the present study, it has been shown that 28% of dopaminergic axon terminals of the NAC in P15 rats contain more than two VGluT2-positive immunogold particles (Dal Bo *et al.*, 2008; Descarries *et al.*, 2008). It is notable that analysis of the same region in adult rats (P90) (Descarries *et al.*, 2008) showed that 12% of TH-positive axon terminals displayed this level of labelling, more than seen in the present study (2% of TH-positive axons contained more than two VGluT2-positive gold particles in the NAC). A more recent study showed a complete lack of VGluT2 labelling in the striatal terminals of mesencephalic dopaminergic neurons of the adult rat (Bérubé-Carrière *et al.*, 2009). Here, we have addressed a concern that VGluT levels may be low in dopaminergic terminals and that previous studies have therefore failed to detect them. By controlling for background levels of labelling, and through comparison with glutamatergic terminals, we show that it is highly unlikely that dopaminergic terminals are expressing even low levels of VGluT2. Moreover, our results extend previous findings by showing no co-expression in the NAS.

The majority of asymmetrical synapses in the dorsal striatum have presynaptic boutons that are immunopositive for either VGluT1 or VGluT2, but about 28% are immunonegative for both (Lacey *et al.*, 2005). Cholinergic interneurons of the striatum, which express VGluT3 in their axon terminals, form symmetrical, not asymmetrical, synapses (Gras *et al.*, 2002; Wainer *et al.*, 1984; Izzo & Bolam, 1988). So, approximately one-third of the excitatory synapses of the striatum are unaccounted for, if indeed they are glutamatergic. This leaves the possibility that another VGluT might exist (e.g. Miyaji *et al.*, 2008; Yarovaya *et al.*, 2005) that is capable of accumulating glutamate in its vesicles at these asymmetrical synapses, but also in dopaminergic neurons. Future studies will no doubt address this possibility, but the present study demonstrates that it is unlikely to be any of the three known VGluTs that perform this function.

The behavioural consequences of the loss of dopamine neurons, whether in animal models as a consequence of the administration of a dopamine neuron toxin or in Parkinson's disease, are alleviated by the administration of therapeutic agents designed to increase activity at dopamine receptors and, indeed, the glutamate receptor antagonist amantadine also has therapeutic benefit in Parkinson's disease (see Lange & Riederer, 1994 for review). One implication of this conclusion is that it is indeed dopamine that is being used to signal rapid reward prediction errors. It is often stated that this signal (with a latency and duration in the order of hundreds of milliseconds) is too fast to be mediated via dopamine (e.g. Chuhma *et al.*, 2004; Lapish *et al.*, 2007). However, glutamatergic synaptic events are so fast that it could be argued they are equally inappropriate to convey this signal. Importantly, dopamine signalling at D2 receptors in the VTA can evoke inhibitory events with a latency and duration in the order of hundreds of milliseconds (Ford *et al.*, 2009), suggesting that, at least under some circumstances, they are capable of signalling the temporal properties of reward prediction errors.

Our data are consistent with an emerging view that dopamine neurons are more likely to co-release glutamate during development, or following injury. For example, the degree of co-localisation of TH

and mRNA for VGluT2 has been reported to be low (19% of TH-positive cells are VGluT2-positive) (Kawano *et al.*, 2006) or only rarely detected (0.3% of VGluT2-positive cells are TH-positive) (Yamaguchi *et al.*, 2007) in the VTA and virtually absent in the substantia nigra and retrorubral field (Kawano *et al.*, 2006) in adult animals. In addition, expression of VGluT2 in the NAC appears to be upregulated when animals are subjected to a neonatal 6-hydroxydopamine lesion (Dal Bo *et al.*, 2008; Descarries *et al.*, 2008). If GABAergic or dopaminergic neurons can suppress the VGluT phenotype in standard cell cultures (Mendez *et al.*, 2008), then it is possible that a lack, or loss, of this suppression in developing or 6-hydroxydopamine-lesioned animals, respectively, enables the expression of the VGluT phenotype. Importantly, the expression of VGluT2 appears to be a consequence of the single-cell microculture, as the inclusion of GABAergic or dopaminergic neurons in the culture results in suppression of the VGluT2 phenotype to levels similar to those seen *in vivo* (Mendez *et al.*, 2008).

Recent studies, however, suggest that glutamatergic synaptic events in the accumbens evoked by VTA stimulation in brain slices do, in fact, come from dopamine neurons (Stuber *et al.*, 2010; Tecuapetla *et al.*, 2010; Hnasko *et al.*, 2010). First, selective stimulation of dopamine neurons in the VTA, using optogenetics, evokes glutamatergic synaptic events in the accumbens (Stuber *et al.*, 2010; Tecuapetla *et al.*, 2010). Second, these events are largely absent following selective deletion of VGluT2 in dopamine neurons (Stuber *et al.*, 2010; Hnasko *et al.*, 2010). How can these findings be reconciled with our anatomical findings and those of others discussed previously? Two caveats should be kept in mind. First, the genetic manipulation of dopamine neurons might induce responses akin to injury or immaturity that could lead to the expression of VGluT2. Second, in dopaminergic terminals in adults, VGluT2 may be expressed at extremely low levels that are not detectable with conventional electron microscopy. It is possible that the functional strength of these glutamatergic synapses also declines with age, although this has not been tested. One interesting possibility that would reconcile the functional and structural data is that dopamine neurons make segregated, glutamatergic synapses that are non-dopaminergic.

In conclusion, we found no evidence for the expression of VGluT1, VGluT2 or VGluT3 in dopaminergic axons and terminals in the DLS and ventral striatum (NAC and NAS). We therefore conclude that, in the normal, adult striatum, dopaminergic synapses do not co-release glutamate, and that the co-release of glutamate by dopamine neurons occurs only during development or following injury, or from segregated, non-dopaminergic synaptic terminals.

## Acknowledgements

This work was supported by the Medical Research Council, UK (grants U138164490 to J. P. Bolam and U120085816 to M. A. Ungless), Parkinson's UK (G-0601 to J. P. Bolam), the European Community (FP7: HEALTH-F2-2008-201716 to J. P. Bolam) and a University Research Fellowship from The Royal Society to M. A. Ungless. J. Moss was supported by a Medical Research Council (UK) studentship. We thank Caroline Francis, Liz Norman, Katie Whitworth and Ben Micklethorp for technical support. We also thank Henrike Hartung, Eleftheria Pissadaki, Pablo Henny and Pete Magill for help at different stages of this project.

## Abbreviations

DAB, diaminobenzidine; DLS, dorsolateral striatum; NAC, nucleus accumbens core; NAS, nucleus accumbens shell; NGS, normal goat serum; P, postnatal day; PBS, phosphate-buffered saline; SEM, standard error of the mean; TH, tyrosine hydroxylase; VGluT, vesicular glutamate transporter; VTA, ventral tegmental area.

## References

- Bellocchio, E.E., Reimer, R.J., Freneau, R.T. Jr & Edwards, R.H. (2000) Uptake of glutamate into synaptic vesicles by an inorganic phosphate transporter. *Science*, **289**, 957–960.
- Bérubé-Carrière, N., Riad, M., Dal Bo, G., Lévesque, D., Trudeau, L.E. & Descarries, L. (2009) The dual dopamine–glutamate phenotype of growing mesencephalic neurons regresses in mature rat brain. *J. Comp. Neurol.*, **517**, 873–891.
- Carlsson, A. (1959) The occurrence, distribution and physiological role of catecholamines in the nervous system. *Pharmacol. Rev.*, **11**, 490–493.
- Chuhma, N., Zhang, H., Masson, J., Zhuang, X., Sulzer, D., Hen, R. & Rayport, S. (2004) Dopamine neurons mediate a fast excitatory signal via their glutamatergic synapses. *J. Neurosci.*, **24**, 972–981.
- Chuhma, N., Choi, W.Y., Mingote, S. & Rayport, S. (2009) Dopamine neuron glutamate cotransmission: frequency-dependent modulation in the mesoventromedial projection. *Neuroscience*, **164**, 1068–1083.
- Dal Bo, G., St-Gelais, F., Danik, M., Williams, S., Cotton, M. & Trudeau, L.E. (2004) Dopamine neurons in culture express VGLUT2 explaining their capacity to release glutamate at synapses in addition to dopamine. *J. Neurochem.*, **88**, 1398–1405.
- Dal Bo, G., Bérubé-Carrière, N., Mendez, J.A., Leo, D., Riad, M., Descarries, L., Lévesque, D. & Trudeau, L.E. (2008) Enhanced glutamatergic phenotype of mesencephalic dopamine neurons after neonatal 6-hydroxydopamine lesion. *Neuroscience*, **156**, 59–70.
- Descarries, L., Bérubé-Carrière, N., Riad, M., Bo, G.D., Mendez, J.A. & Trudeau, L.E. (2008) Glutamate in dopamine neurons: synaptic versus diffuse transmission. *Brain Res. Rev.*, **58**, 290–302.
- Ford, C.P., Phillips, P.E. & Williams, J.T. (2009) The time course of dopamine transmission in the ventral tegmental area. *J. Neurosci.*, **29**, 13344–13352.
- Freneau, R.T. Jr, Troyer, M.D., Pahner, I., Nygaard, G.O., Tran, C.H., Reimer, R.J., Bellocchio, E.E., Fortin, D., Storm-Mathisen, J. & Edwards, R.H. (2001) The expression of vesicular glutamate transporters defines two classes of excitatory synapse. *Neuron*, **31**, 247–260.
- Freneau, R.T. Jr, Burman, J., Qureshi, T., Tran, C.H., Proctor, J., Johnson, J., Zhang, H., Sulzer, D., Copenhagen, D.R., Storm-Mathisen, J., Reimer, R.J., Chaudhry, F.A. & Edwards, R.H. (2002) The identification of vesicular glutamate transporter 3 suggests novel modes of signaling by glutamate. *Proc. Natl Acad. Sci. USA*, **99**, 14488–14493.
- Fujiyama, F., Kuramoto, E., Okamoto, K., Hioki, H., Furuta, T., Zhou, L., Nomura, S. & Kaneko, T. (2004) Presynaptic localization of an AMPA-type glutamate receptor in corticostriatal and thalamostriatal axon terminals. *Eur. J. Neurosci.*, **20**, 3322–3330.
- Gras, C., Herzog, E., Bellenchi, G.C., Bernard, V., Ravassard, P., Pohl, M., Gasnier, B., Giros, B. & El Mestikawy, S. (2002) A third vesicular glutamate transporter expressed by cholinergic and serotonergic neurons. *J. Neurosci.*, **22**, 5442–5451.
- Hanley, J.J. & Bolam, J.P. (1997) Synaptology of the nigrostriatal projection in relation to the compartmental organization of the neostriatum in the rat. *Neuroscience*, **81**, 353–370.
- Herzog, E., Gilchrist, J., Gras, C., Muzerelle, A., Ravassard, P., Giros, B., Gaspar, P. & El Mestikawy, S. (2004) Localization of VGLUT3, the vesicular glutamate transporter type 3, in the rat brain. *Neuroscience*, **123**, 983–1002.
- Hnasko, T.S., Chuhma, N., Zhang, H., Goh, G.Y., Sulzer, D., Palmiter, R.D., Rayport, S. & Edwards, R.H. (2010) Vesicular glutamate transport promotes dopamine storage and glutamate corelease in vivo. *Neuron*, **65**, 643–656.
- Izzo, P.N. & Bolam, J.P. (1988) Cholinergic synaptic input to different parts of spiny striatonigral neurons in the rat. *J. Comp. Neurol.*, **269**, 219–234.
- Joyce, M.P. & Rayport, S. (2000) Mesoaccumbens dopamine neuron synapses reconstructed in vitro are glutamatergic. *Neuroscience*, **99**, 445–456.
- Kaneko, T., Akiyama, H., Nagatsu, I. & Mizuno, N. (1990) Immunohistochemical demonstration of glutaminase in catecholaminergic and serotonergic neurons of rat brain. *Brain Res.*, **507**, 151–154.
- Kawano, M., Kawasaki, A., Sakata-Haga, H., Fukui, Y., Kawano, H., Nogami, H. & Hisano, S. (2006) Particular subpopulations of midbrain and hypothalamic dopamine neurons express vesicular glutamate transporter 2 in the rat brain. *J. Comp. Neurol.*, **498**, 581–592.
- Kitai, S.T., Kocsis, J.D., Preston, R.J. & Sugimori, M. (1976) Monosynaptic inputs to caudate neurons identified by intracellular injection of horseradish peroxidase. *Brain Res.*, **109**, 601–606.
- Lacey, C.J., Boyes, J., Gerlach, O., Chen, L., Magill, P.J. & Bolam, J.P. (2005) GABA(B) receptors at glutamatergic synapses in the rat striatum. *Neuroscience*, **136**, 1083–1095.
- Lange, K.W. & Riederer, P. (1994) Glutamatergic drugs in Parkinson's disease. *Life Sci.*, **55**, 2067–2075.
- Lapish, C.C., Kroener, S., Durstewitz, D., Lavin, A. & Seamans, J.K. (2007) The ability of the mesocortical dopamine system to operate in distinct temporal modes. *Psychopharmacology (Berl.)*, **191**, 609–625.
- Mendez, J.A., Bourque, M.J., Dal Bo, G., Bourdeau, M.L., Danik, M., Williams, S., Lacaille, J.C. & Trudeau, L.E. (2008) Developmental and target-dependent regulation of vesicular glutamate transporter expression by dopamine neurons. *J. Neurosci.*, **28**, 6309–6318.
- Miyaji, T., Echigo, N., Hiasa, M., Senoh, S., Omote, H. & Moriyama, Y. (2008) Identification of a vesicular aspartate transporter. *Proc. Natl Acad. Sci. USA*, **105**, 11720–11724.
- Moore, R.Y. & Card, J.P. (1984). Noradrenaline-containing neuron systems. In Bjorklund, A. & Hokfelt, T. (Eds), *Handbook of chemical neuroanatomy, vol. 2: classical transmitters in the CNS Part 1*. Elsevier, Amsterdam, pp. 123–156.
- Moss, J. & Bolam, J.P. (2008) A dopaminergic axon lattice in the striatum and its relationship with cortical and thalamic terminals. *J. Neurosci.*, **28**, 11221–11230.
- Moss, J. & Bolam, J.P. (2009a) Dopaminergic axons in the adult rat striatum do not express vesicular glutamate transporters. *Br. Neurosci. Assoc. Abstr.*, **20**, 32.
- Moss, J. & Bolam, J.P. (2009b) *Dopaminergic axons in the adult rat striatum do not express vesicular glutamate transporters*. Program No. 845.15.2009. Neuroscience Meeting Planner. Society for Neuroscience, Chicago, IL. Online.
- Nair-Roberts, R.G., Chatelain-Badie, S.D., Benson, E., White-Cooper, H., Bolam, J.P. & Ungless, M.A. (2008) Stereological estimates of dopaminergic, GABAergic and glutamatergic neurons in the ventral tegmental area, substantia nigra and retrorubral field in the rat. *Neuroscience*, **152**, 1024–1031.
- Paxinos, G. & Watson, C.R.R. 2007. *The Rat Brain in Stereotaxic Coordinates*. Elsevier, Amsterdam.
- Rayport, S. (2001) Glutamate is a cotransmitter in ventral midbrain dopamine neurons. *Parkinsonism Relat. Disord.*, **7**, 261–264.
- Schultz, W. (1998) Predictive reward signal of dopamine neurons. *J. Neurophysiol.*, **80**, 1–27.
- Stuber, G.D., Hnasko, T.S., Britt, J.P., Edwards, R.H. & Bonci, A. (2010) Dopaminergic terminals in the nucleus accumbens but not the dorsal striatum corelease glutamate. *J. Neurosci.*, **30**, 8229–8233.
- Sulzer, D. & Rayport, S. (2000) Dale's principle and glutamate corelease from ventral midbrain dopamine neurons. *Amino Acids*, **19**, 45–52.
- Sulzer, D., Joyce, M.P., Lin, L., Geldwert, D., Haber, S.N., Hattori, T. & Rayport, S. (1998) Dopamine neurons make glutamatergic synapses in vitro. *J. Neurosci.*, **18**, 4588–4602.
- Takamori, S., Rhee, J.S., Rosenmund, C. & Jahn, R. (2001) Identification of differentiation-associated brain-specific phosphate transporter as a second vesicular glutamate transporter (VGLUT2). *J. Neurosci.*, **21**, RC182, 1–6.
- Tecuapetla, F., Patel, J.C., Xenias, H., English, D., Tadros, I., Shah, F., Berlin, J., Deisseroth, K., Rice, M.E., Tepper, J.M. & Koos, T. (2010) Glutamatergic signaling by mesolimbic dopamine neurons in the nucleus accumbens. *J. Neurosci.*, **30**, 7105–7110.
- Wainer, B.H., Bolam, J.P., Freund, T.F., Henderson, Z., Totterdell, S. & Smith, A.D. (1984) Cholinergic synapses in the rat brain: a correlated light and electron microscopic study employing a monoclonal antibody against choline acetyltransferase. *Brain Res.*, **308**, 69–76.
- Yamaguchi, T., Sheen, W. & Morales, M. (2007) Glutamatergic neurons are present in the rat ventral tegmental area. *Eur. J. Neurosci.*, **25**, 106–118.
- Yarovaya, N., Schot, R., Fodero, L., McMahon, M., Mahoney, A., Williams, R., Verbeek, E., de Bondt, A., Hampson, M., van der Spek, P., Stubbs, A., Masters, C.L., Verheijen, F.W., Mancini, G.M. & Venter, D.J. (2005) Sialin, an anion transporter defective in sialic acid storage diseases, shows highly variable expression in adult mouse brain, and is developmentally regulated. *Neurobiol. Dis.*, **19**, 351–365.